Study on the Foaming of $CaO-SiO_2-FeO$ Slags: Part I. Foaming Parameters and Experimental Results

KIMIHISA ITO and R.J. FRUEHAN

In order to understand the effect of slag composition on foaming in iron and steelmaking processes, slag foaming was quantitatively studied for $CaO-SiO_2-FeO$ slags in the temperature range of 1250 °C to 1400 °C. It was found that slag foaming could be characterized by a foaming index (Σ), which is equal to the retention or traveling time of the gas in the slag, and the average foam life (τ). The effects of P_2O_5, S, MgO, and CaF_2 on foaming were studied. As expected, slag foaming increased with increasing viscosity and decreasing surface tension. It was found that suspended second-phase solid particles such as CaO, $2CaO \cdot SiO_2$, and MgO stabilized the foam and had a larger effect on foaming than changes in viscosity and surface tension for the slags studied.

I. INTRODUCTION

THE foaming phenomenon of molten slags in metallurgical processes has been observed and studied for a long time. Most of the early practical work on slag foaming was carried out to reduce or eliminate the foam in oxygen steelmaking furnaces, because the foamed slag prevents proper operation. On the other hand, the basic research on foaming was limited to a qualitative understanding of this complex phenomenon. Recently, slag foaming has become important not only for basic oxygen furnace (BOF) steelmaking but also for the modern electric arc furnace (EAF) and the new ironmaking processes (*i.e.*, bath smelting). In modern electric furnace steelmaking, foaming practices are being widely used to shield the refractories from the arc. The foamed slag also stabilizes the arc and shields the metal from the atmosphere. The control of foaming height is required to maintain a steady operation. In the bath-smelting process currently being developed (smelting reduction), coal and iron oxide are injected into an iron bath; the main reactions are the cracking of the coal and the reduction of iron oxide in slag by solid carbon and carbon dissolved in metal. Therefore, a large amount of CO and H_2 gas is evolved when a high production rate is maintained, and violent foaming will be inevitable. On the other hand, the foamed slag plays an important role in heat transfer from the post-combustion flame to the metal in the process reactor. Therefore, the control of foaming is critical for these new processes.

Since the prediction and control of slag foaming are required for current and future iron and steelmaking processes, a quantitative study of foaming is important. However, in previous work,[1-4] foaming was described in terms of the surface chemistry, whereas foaming is a dynamic phenomenon of a special case of one-dimensional two-phase flow.[5] A quantitative prediction about foaming in practical operations using the previous work is difficult, because slag foaming was expressed as an arbitrarily defined foam life.

Cooper and Kitcher[1] studied the foaming of $CaO-SiO_2$ slags at temperatures ranging from 1475 °C to 1725 °C. The CaO/SiO_2 ratio of the slag was less than 0.9. They measured the life of a given volume of foam, and therefore, it was a dynamic foaming index. The foam life increased with decreasing temperature and decreasing basicity. The addition of small amounts of P_2O_5 significantly increased foam life. Swisher and McCabe[2] studied the effect of Cr_2O_3 on the foaming of $CaO-SiO_2$ slags in the temperature range of 1580 °C to 1640 °C by using the same technique employed by Cooper and Kitcher. The CaO/SiO_2 ratio was less than 0.8. They reported that Cr_2O_3 increased the foam life within the completely liquid region of slag compositions. The foaming phenomenon from the surface-chemical point of view has been discussed in detail by Kozakevitch.[3] Hara *et al.*[4] recently measured the foam life and foam height for $CaO-FeO$, SiO_2-FeO, and $CaO-SiO_2-FeO$ systems at 1250 °C and 1300 °C. The CaO/SiO_2 ratio of the ternary slag was less than 1.0. The foam life was defined in the same manner as in the previous studies. They found a good correlation between the foam life, foam height, and surface tension of the slag. The effect of P_2O_5, Na_2O, Cr_2O_3, and CaF_2 on the foam stability was also reported. Kleppe and Oeters[6] studied the foaming by using a hydrodynamic model; however, these results are difficult to extrapolate to iron and steelmaking systems.

It is the purpose of the present study to measure slag foaming for $CaO-SiO_2-FeO$ slags relevant to iron and steelmaking processes. The effect of CaS, P_2O_5, CaF_2, and MgO, commonly found in slags, on foaming is also determined. In doing so, foaming parameters must be developed which reflect the foamability of the slag which can be extrapolated to actual conditions. In Part II of this paper, a dimensional analysis is performed to extrapolate the results to other slag compositions, and predictions of slag foaming in oxygen steelmaking, electric furnace steelmaking, and bath smelting are made.

KIMIHISA ITO, Research Associate, formerly with the Department of Metallurgical Engineering and Materials Science, Carnegie Mellon University, is with the Research Institute of Mineral Dressing and Metallurgy, Tohoku University, Sendai, Japan. R.J. FRUEHAN, Professor, is with the Department of Metallurgical Engineering and Materials Science, Carnegie Mellon University, Pittsburgh, PA 15213.

Manuscript submitted May 19, 1988.

II. EXPERIMENTAL PROCEDURES

A schematic drawing of the experimental setup is shown in Figure 1. An electric resistance furnace with a 150-mm hot zone length was used for the experiments to establish an isothermal condition. The slag was prepared from CaO, SiO_2, and FeO. The slag was contained in an alumina crucible (i.d. = 32 to 50 mm; H = 200 mm) and foamed by injection argon. The argon gas was introduced into the molten slag through a stainless steel pipe with a knife edged nozzle (d. = 2.1 mm at 1573 K). The surface position of the slag was detected by an electric probe made of a stainless steel rod. The foam height was defined as the increment of the slag surface level from the original (*i.e.*, gas flowrate is zero) slag surface to the foaming slag surface. The mean bubble size was calculated from the gas flowrate and the bubble formation frequency, which was determined using a pressure transducer connected to the bubbling nozzle. Although the surface position of the foamed slag was periodically moving up and down due to the rupturing of the bubbles, the measured value for the maximum surface level showed good reproducibility. Therefore, the maximum surface position from the original surface was defined as foam height (h (cm)). The wall of the crucible was coated with the slag before the experiment to reduce the wall effects by foaming the slag for 10 to 15 minutes prior to any measurements. The crucible material, alumina, dissolved into the slag during the experiments. Therefore, the slag was analyzed after each experiment; the amount of alumina after the end of an experiment was usually 3 to 5 wt pct.

III. RELATIONSHIPS FOR FOAMING PARAMETERS

A. *Foaming Index*

In the present work, the foaming index (Σ) is defined as follows by modifying the foaming index used in the aqueous foams.[7,8] Figure 2 shows a schematic drawing

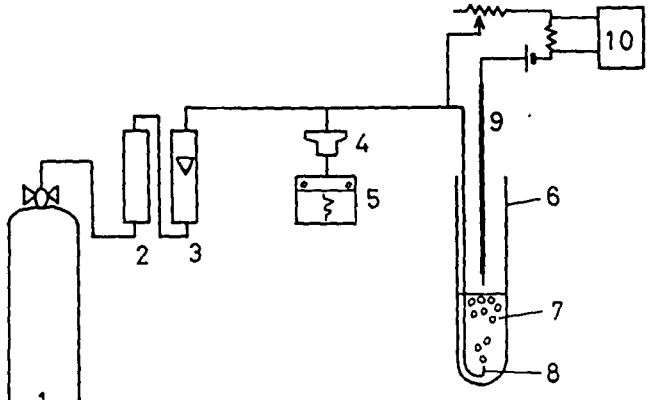

Fig. 1—Schematic drawing of the experimental apparatus.

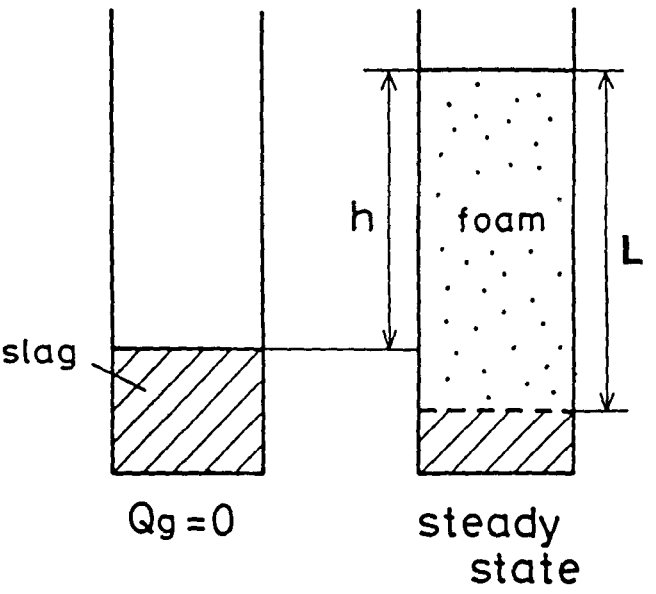

Fig. 2—Illustration of slag foaming.

of the foamed slag. The superficial gas velocity (V_g^s (cm/s)) is defined by Eq. [1], and the average gas traveling time or foaming index (Σ) is defined by Eq. [2].

$$V_g^s = \frac{Q_g}{A} \quad [1]$$

$$\Sigma = \frac{\Delta h}{\Delta V_g^s} \quad [2]$$

where Q_g (cm^3/s) is the gas flowrate, A is the cross-section area of the container, and Δh is the change of slag height.

The superficial gas velocity (V_g^s) is also correlated to the void fraction (α), the volumetric fraction of gas, and the actual gas velocity (V_g (cm/s)) by Eq. [3].

$$V_g^s = \alpha V_g \quad [3]$$

The foam height (h) is expressed as a function of void fraction (α) and foam layer thickness (L (cm)) in Eq. [4].

$$h = \alpha L \quad [4]$$

Finally, Σ is expressed in Eq. [5] in terms of the foam layer thickness (L) and the actual gas velocity (V_g).

$$\Sigma = \frac{\Delta L}{\Delta V_g} \quad [5]$$

From Eq. [5], it is clear that Σ means the average gas traveling time through the foamed layer.

The above equations are valid when α is independent of foam height. The void fraction profile in the foam was previously measured by using an electrical sensor, AD converter, and microcomputer system. The void fraction was between 0.7 and 0.9 and almost independent of position in the foam.[9] Therefore, α can be assumed to be constant.

B. *Foam Life*

If the formation of foam is proportional to the gas flowrate and the rupture of foam is proportional to its

height, the rate equation for the change in foam height can be written in Eq. [6].

$$\frac{dh}{dt} = K_1 Q_g - K_2 h \quad [6]$$

where K_1 and K_2 are the formation and rupture constants of foam, respectively. When the system is in the steady state,

$$\frac{dh}{dt} = 0 \quad [7]$$

Therefore,

$$K_1 Q_g = K_2 h \quad [8]$$

On the other hand, if the gas is stopped (*i.e.*, $Q_g = 0$) at the steady state, Eq. [6] reduces to

$$\frac{dh}{dt} = -K_2 h \quad [9]$$

Integrating Eq. [9] from $t = 0$ to $t = t$ and from $h = h^0$ to $h = h$ gives the foam height as a function of time.

$$K_2 t = -\ln\left(\frac{h}{h^0}\right) \quad [10]$$

The rupture of foam is expressed as the drainage of the liquid in the foam. The rate equation of drainage is given by Eq. [11], assuming a first-order drainage rate.[7]

$$\frac{dv}{dt} = k(V^0 - v) \quad [11]$$

where V^0 (cm^3) is the initial liquid volume in foam and v (cm^3) is the drained liquid volume. Integrating of Eq. [11] from $t = 0$ gives

$$kt = -\ln\left\langle\frac{V^0 - v}{V^0}\right\rangle \quad [12]$$

Since the void fraction is almost constant, Eq. [12] can be written as follows:

$$kt = -\ln\left(\frac{h}{h^0}\right) \quad [13]$$

The average foam life (τ) is obtained in Eq. [14].

$$\tau = \frac{1}{V^0}\int_0^{v^0} t\,dv$$

$$= k\int_0^{\infty} te^{-kt}\,dt = \frac{1}{k} \quad [14]$$

From Eqs. [10] and [12] it is obvious that the rupture constant K_2 and the drainage constant k are the same and are correlated to the foam life by Eq. [14]. Therefore, if the decay of the foam height was measured and $-\ln(h/h^0)$ is plotted against time, the gradient will be the foam life. In the experiment, the time required to reduce the foam height from h^0 to the specified position h was measured after stopping the gas injection and maintaining the steady state (*i.e.*, foam height is equal to h^0).

C. *Relation between Foaming Index and Foam Life*

For an ideal system, for which α is constant, the foaming index Σ can be related to the foam life τ. The formation of foam is written in Eq. [15], assuming α is constant.

$$\frac{dh}{dt} = \alpha\frac{dL}{dt} = \frac{\alpha}{A}\frac{dV^{\text{foam}}}{dt} = \frac{Q_g}{A} \quad [15]$$

where V^{foam} (cm^3) is a volume of foam.

Since α is constant, Eq. [16] is obtained from Eq. [15] with Eq. [6].

$$K_1 = \frac{1}{A} \quad [16]$$

From Eqs. [8], [14], and [16], the following relationship is obtained:

$$\frac{\tau}{A} = \frac{h}{Q_g} \quad [17]$$

The foaming can be related to the foam life in Eq. [18] using Eqs. [1], [2], and [17].

$$\tau = \frac{\Delta h}{\Delta(Q_g/A)} = \Sigma \quad [18]$$

Therefore, for an "ideal slag," the foaming index Σ is equal to the average foam life τ.

IV. EXPERIMENTAL RESULTS AND DISCUSSION

A. *Bubble Size*

Figure 3 shows the measured bubble diameter as a function of gas flowrate. The measured bubble diameter is in good agreement with that calculated from the equation proposed by Sano and Mori[10] shown as a line in Figure 3. The addition of 1 wt pct P_2O_5 decreased the

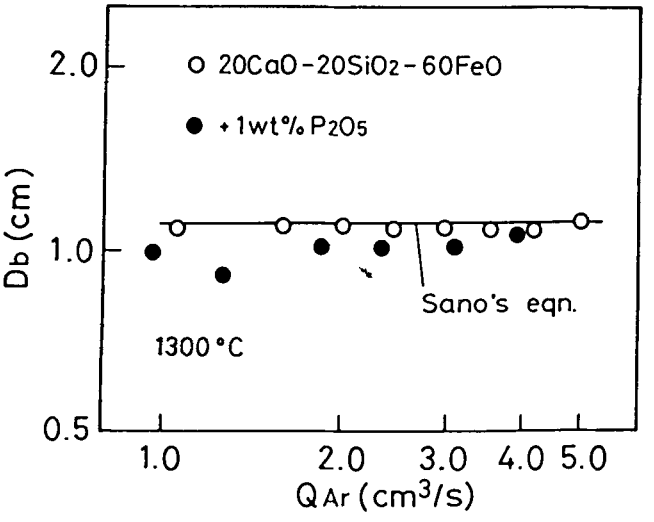

Fig. 3—The relation between mean bubble diameter and gas flowrate at 1573 K.

bubble diameter, because P_2O_5 decreases the surface tension of the slag. The bubble diameter could not be accurately determined when the gas flowrate exceeded 15 cm^3/s, because the bubble frequency was too high. For these cases, Sano and Mori's equation was used to calculate the bubble size. For all the experiments, the bubble diameter in the foamed layer ranged from 10 to 15 mm.

B. *Foaming Index*

The relation between foam height (h) and gas flowrate is shown in Figure 4 for crucibles of varying diameter. The foam height increases with increasing gas flowrate for every case. For the same gas flowrate (Q_g), the smaller the crucible diameter, the larger the foam height.

Figure 5 shows the dependency of foam height (h) and the average gas traveling time in the foaming slag (Σ) on the superficial gas velocity (V_g^s). The foam height increased linearly with the increasing (V_g^s), and Σ becomes constant after a certain flowrate is reached. If the diameter of the crucible was larger than 32 mm, the results are all on the same line, indicating Σ is independent of crucible diameter and wall effects are small. Therefore, Σ can be used as a characteristic foaming index. In most experiments, crucibles with 32- and 38-mm diameters were used for experimental convenience.

C. *Foam Life*

Typical results for foam life measurements are shown in Figure 6. A good linear relationship was obtained between time (s) and $-\ln(h/h^0)$, as predicted by Eq. [14]. The lines do not pass the origin, because the bubble formation continued for a short time after closing the valve; *i.e.*, time $t = 0$ is ill-defined. However, the lines all have the same intercept, showing consistency.

D. *Effect of Basicity*

Figure 7 shows the foaming index and foam life for $CaO\text{-}SiO_2\text{-}FeO$ slags at 1573 K as a function of basicity

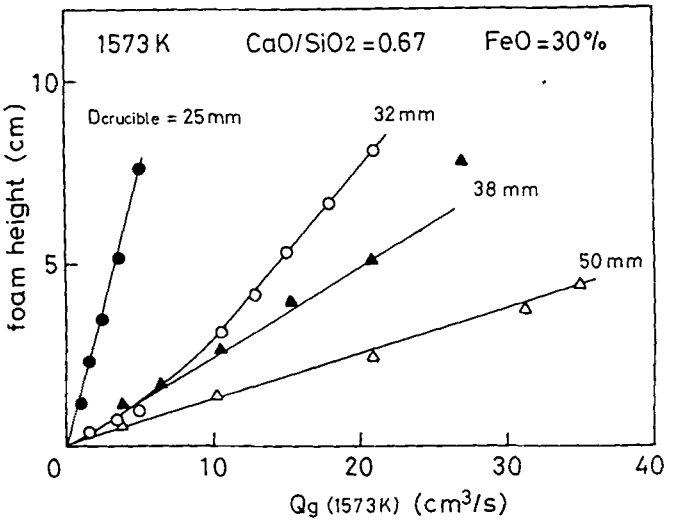

Fig. 4—The relation between foam height and gas flowrate for various crucible sizes.

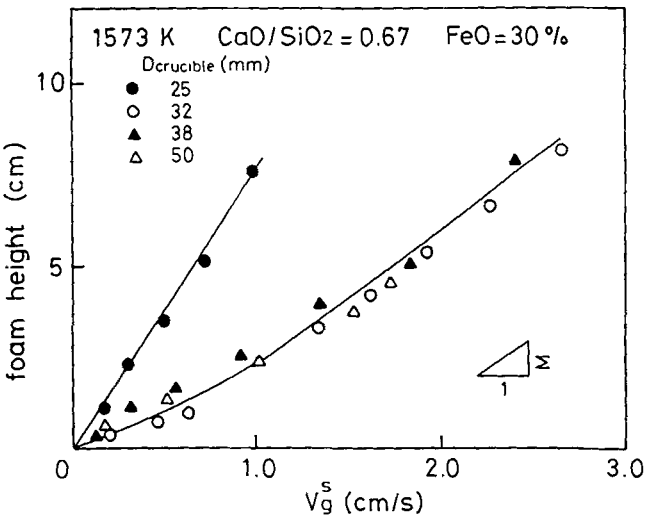

Fig. 5—The relation between foam height and superficial gas velocity for various crucible sizes.

index in weight percent ($CaO/(SiO_2 + Al_2O_3)$). Both Σ and τ decrease with increasing basicity, because high basicity slags have higher surface tension and lower viscosity which destabilize the foam. It is also indicated in Figure 7 that τ and Σ have approximately the same value, and considering the experimental error, it can be concluded that the assumptions involved in obtaining Eq. [18]

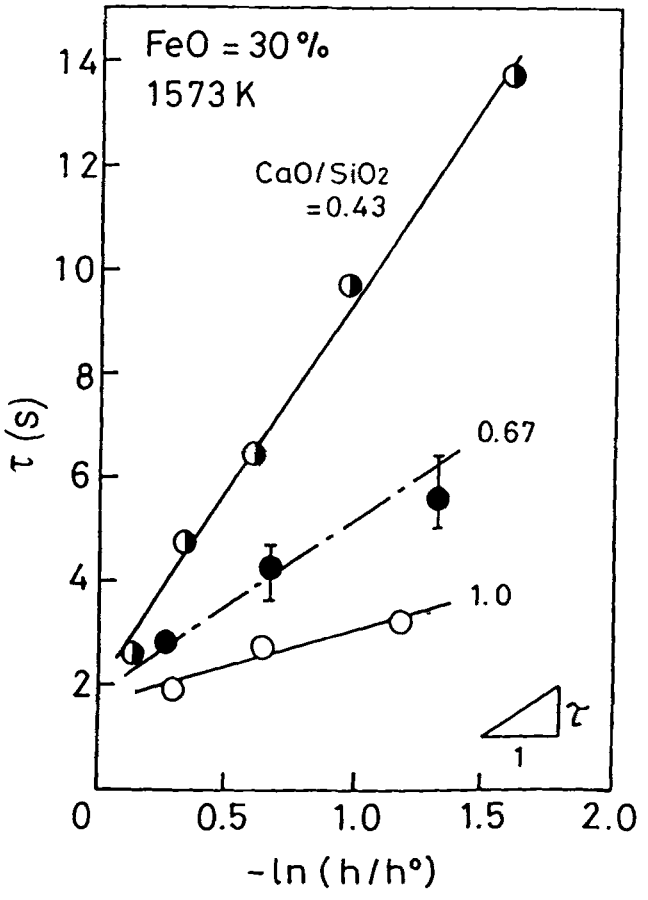

Fig. 6—The relation between $-\ln(h/h^0)$ and time (s).

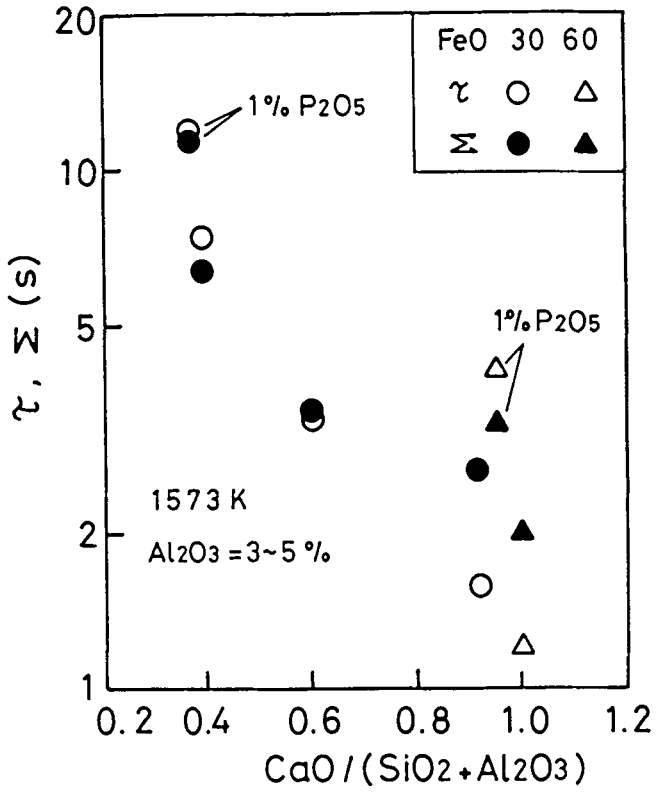

Fig. 7—The change of foaming index Σ and foam life τ with basicity index (CaO/SiO_2) of the $CaO-SiO_2$-FeO slag.

are reasonable. The small differences in τ and Σ are primarily due to experimental scatter and the assumptions for an ideal foam, *i.e.*, first low drainage rate and constant void fraction.

E. *Effect of Second-Phase Particles*

The effect of the presence of the second-phase particle was measured by adding $2CaO \cdot SiO_2$ or CaO particles (diameter 30 to 100 μm) to the slag. Figure 8 shows the relationship between the volumetric particle concentration and foaming where Σ^0 is the foaming index without second-phase particles for that particular slag. The value of Σ increases with increasing particle concentration. If it is assumed for the case of the CaO addition that all the CaO formed $2CaO \cdot SiO_2$, the volume of the second-phase particles would increase, and those points would also fall on the line for the $2CaO \cdot SiO_2$ particles.

Figure 9 shows the foaming index (Σ) as a function of slag basicity defined as wt pct CaO/wt pct SiO_2. The Σ decreases with increasing CaO/SiO_2 up to $CaO/SiO_2 = 1.20$ at 1573 K and 1.22 at 1673 K, which are the liquidus compositions. The surface tension increases and viscosity decreases with increasing CaO. Therefore, low surface tension and high viscosity stabilized the slag foam. However, Σ increased with increasing CaO/SiO_2 when CaO/SiO_2 was in excess of the liquidus composition. This is because solid particles such as $2CaO \cdot SiO_2$ precipitate at higher CaO contents, and the particles significantly increase foam stability. Therefore, the precipitation of second-phase particles has a larger effect than the increase in surface tension and decrease in viscosity on foam stability for these slags.

F. *Effects of S, P, CaF_2, and MgO*

Figure 10 shows the effect of additions of S, P_2O_5, CaF_2, and MgO on the foaming index at 1673 K. In Figure 10, Σ^0 is the foam index for the slag without the additive. The P and S are surface active components which lower the surface tension of the slag. P_2O_5 slightly increases Σ, whereas sulfur marginally decreases Σ. This indicates that surface tension alone does not have a great effect on slag foamability. In general, CaF_2 decreased Σ by lowering the viscosity of the slag. Larger additions of CaF_2 significantly decrease the foam stability by increasing CaO solubility and, consequently, dissolving some of the second-phase particles. The MgO increases Σ, probably because it increases the amount of solid particles in the slag. However, the amount of solid particles in the slag in this case could not be estimated, because the phase diagram for a $CaO-SiO_2$-FeO-MgO system is unknown.

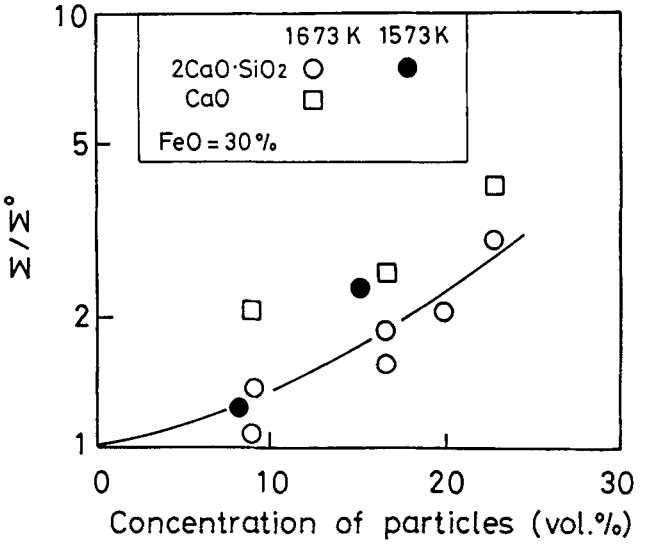

Fig. 8—The relation between foaming index Σ and the basicity index of $CaO-SiO_2$-FeO slags.

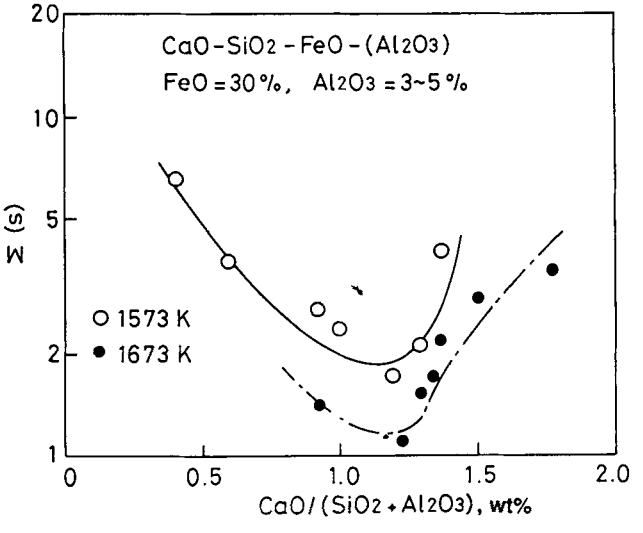

Fig. 9—The effect of the second-phase particles such as CaO and $2CaO \cdot SiO_2$ on the foaming index.

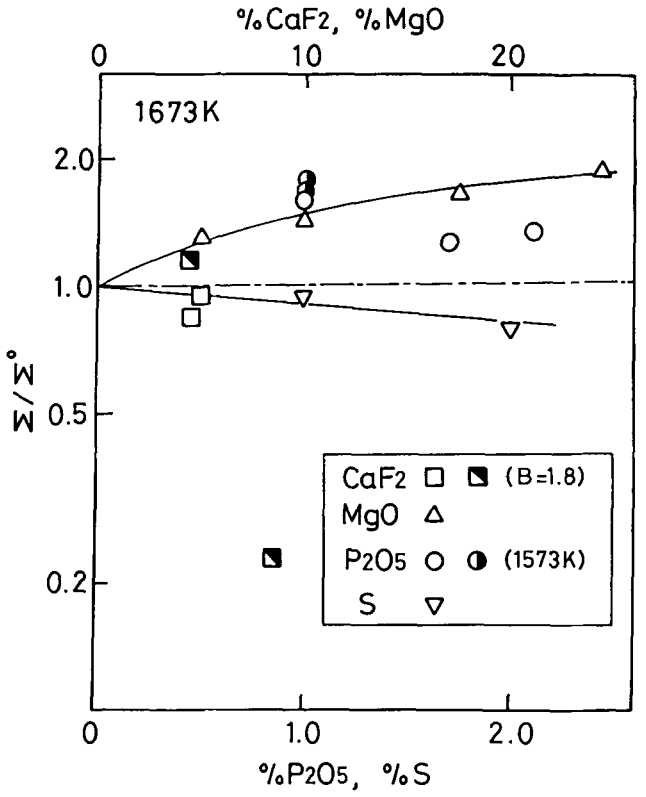

Fig. 10—The effect of CaF_2, P_2O_5, S, and MgO on the foaming index.

G. *Temperature Dependence*

Figure 11 shows the temperature dependency of the foaming index for a 35 pct CaO-35 pct SiO_2-30 pct FeO slag; log (Σ) is inversely proportional to temperature. When the temperature drops from 1350 °C to 1250 °C, Σ increases by a factor of two. Since the temperature coefficient for surface tension[11] is positive and that for viscosity[12] is negative, decreasing temperature would be expected to stabilize the foam as observed. The temperature dependency in Σ, in terms of an activation energy, is 160 kJ, which is almost the same as that for the viscosity for these slags. The temperature dependency of foam life for a CaO-SiO_2 system measured by Kitcher[1] was larger than that obtained in the present study. However, that definition of foam life is different from Eq. [11], and the temperature range was also different.

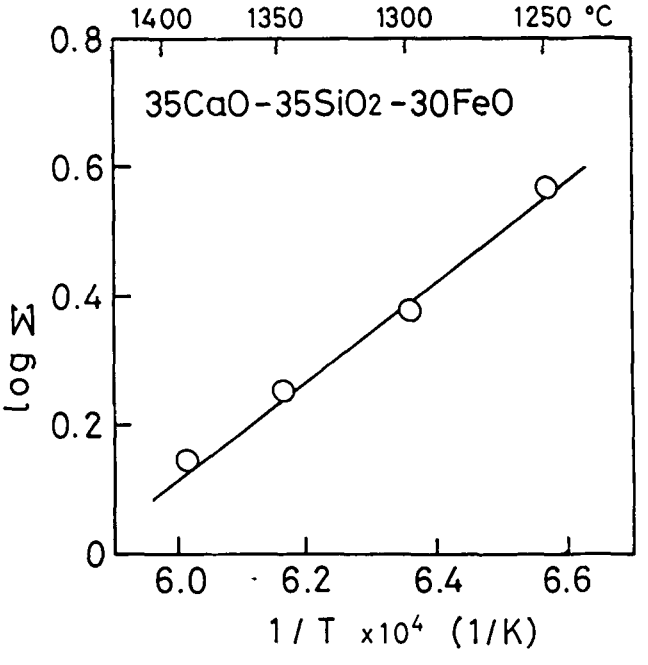

Fig. 11—The temperature dependency of the foaming index for a 35 pct CaO-35 pct SiO_2-30 pct FeO slag.

V. SUMMARY AND CONCLUSIONS

Slag foaming is an important factor in existing processes and may be extremely so for the new in-bath smelting process for producing iron. However, in previous studies, slag foaming was very qualitatively studied. In the present study, the major findings were:

1. The slag foaminess was quantitatively characterized by the average gas traveling time (Σ) and average foam life (τ). It is shown that for an "ideal slag," these quantities are equal.
2. In a CaO-SiO_2-FeO system, the Σ decreased with the increasing basicity up to 1.22 at 1400 °C; when CaO/SiO_2 was greater than 1.22, Σ increased due to the presence of second-phase particles (CaO or $2CaO \cdot SiO_2$). Second-phase particles have a large effect on foam stability.
3. P_2O_5 slightly increased Σ, whereas CaS marginally decreased Σ. CaF_2 decreased Σ by lowering viscosity of the slag.
4. Σ decreased with increasing temperature because of the decrease of viscosity and the increase of surface tension.

In Part II of this paper, the results are examined by dimensional analysis, and predictions are made for slag foaming in actual processes.

ACKNOWLEDGMENTS

Support of this work by the National Science Foundation under Grant No. 8713941 and the member companies of the Center for Iron and Steelmaking Research is gratefully acknowledged.

REFERENCES

1. C.F. Cooper and J.A. Kitcher: *JISI*, Sept. 1959, vol. 193, pp. 48-55.
2. J.H. Swisher and C.L. McCabe: *Trans. TMS-AIME*, Dec. 1964, vol. 230, pp. 1669-75.
3. P. Kozakevitch: *J. Metals*, July 1969, pp. 57-68.
4. S. Hara, M. Ikuta, M. Kitamura, and M. Ogino: *Tetsu-to-Hagané*, 1983, vol. 69 (9), pp. 1152-59.
5. Graham B. Wallis: *One-Dimensional Two-Phase Flow*, McGraw-Hill, New York, NY, 1969, pp. 243-81.
6. W. Kleppe and F. Oeters: *Arch. Eisenhüttenwes.*, 1977, vol. 48, pp. 193-97.
7. J.J. Bikerman: *Foams*, Springer-Verlag, New York, NY, 1973, pp. 65-97 and 149-58.
8. B.J. Akers: *Foams*, Academic Press, London, 1976, pp. 1-38.
9. K. Ito and R.J. Fruehan: Carnegie Mellon University, Pittsburgh, PA, unpublished research, 1987.
10. M. Sano and K. Mori: *Tetsu-to-Hagané*, 1977, vol. 63 (14), pp. 2308-15.
11. Y. Kawai, K. Mori, H. Shiraishi, and N. Yamada: *Tetsu-to-Hagané*, 1976, vol. 62 (1), pp. 53-61.
12. P. Kozakevitch: *Rev. Met.*, 1949, vol. 46, pp. 505-15.